JOURNAL OF MATERIALS SCIENCE **35** (2000) 837–850

Microstructures of *in situ* Al/TiB_2 MMCs prepared by a casting route

C. F. FENG*, L. FROYEN
Department of Metallurgy and Materials Engineering, Katholieke Universiteit Leuven, de Croylaan 2, B-3001 Leuven, Belgium
E-mail: mcffeng@ntu.edu.sg

In situ Al/TiB_2 metal matrix composites (MMCs) have been successfully produced by Salt-Metal reactions. This is a novel low-cost reactive approach, which involves adding Ti and B bearing salts to molten Al. The reactions between the salts lead to the formation of the reinforcing TiB_2 particles in the Al matrix. The *in situ* formed TiB_2 particles are very fine (below $\sim$1 μm in size). Strings and clusters of particle agglomerates are distinct microstructural features of all the composites with pure Al as the matrix. The effects of processing parameters on the kinetics of TiB_2 formation and on the final microstructures are studied in detail. Besides, efforts are made to improve the distribution of TiB_2 particles in the Al matrix by means of chemical additions; it is found that a homogeneous distribution is obtained by using a eutectic Al-Si alloy as the matrix material.

1. Introduction

For preparing metal matrix composites (MMCs), *in situ* processing offers significant advantages over the conventional processing from both technical and economic standpoints. The technique of Salt-Metal reactions is an attractive *in situ* approach developed typically for preparing Al/TiB_2 MMCs. It involves adding mixed Ti and B bearing salts (i.e. $K_2TiF_6 + KBF_4$) to molten aluminium, giving rise to the formation of a dispersion of TiB_2 particles in the Al matrix. This process for developing MMCs is based on a well-established technology for producing Al-Ti-B master alloys for the grain refining industry of aluminium. The technology uses the reaction between molten salts to produce TiB_2 *in situ* within molten aluminium. The master alloys comprise a fine distribution of TiB_2 in aluminium but at a very dilute level (typically less than 3 vol%). A patent (UK 2259 308A) has been applied for to use the same technology to form higher loading of TiB_2 in aluminium. Davies *et al.* claims that the products would combine high strength with good ductility and would be competitive both technically and economically with existing cast MMCs [1]. This actually provides a novel low-cost route for fabricating a type of useful composite. The applications of this type of material are foreseen in different parts of the automotive and aerospace industrials.

The TiB_2 particles, *in situ* formed in the matrix of pure Al, are very fine in size (below $\sim$1 μm in size). They generally stick together appearing as strings or clusters of particle agglomerates, leading to an inhomogeneous distribution. At present no literature can be found reporting on the achievement of agglomeration-free TiB_2 particles. In order to obtain a useful composite with good properties, we have to achieve less agglomeration and more uniform distribution of the TiB_2 particles. One approach for this purpose is to find a suitable alloying element for the matrix aluminium which could positively modify the interface properties between TiB_2 and Al.

The objective of this paper is twofold. The first it to study the influences of processing parameters on the kinetics of TiB_2 formation as well as on the microstructure of the composite products. The second is to improve the dispersion of TiB_2 by means of chemical additions in the aluminium matrix.

2. Experimental

2.1. Materials

The salt powders K_2TiF_6 and KBF_4 were both purchased from the Aldrich Chemical Company, Inc., USA. The particles of the two different sorts are irregularly shaped (Fig. 1). Commercial pure Al blocks (99.5%) were used as base metal to synthesise Al/TiB_2 MMCs. In the study to improve the dispersion, Al binary alloys were used as the base metal for processing the *in situ* composites. The investigated alloying elements were Mg, Sb, Mn, Cu, Zn, Fe, Cr and Si. Among the binary Al alloys, Al-10wt% Mn and Al-12wt%Si were available as starting alloys. The other alloys were prepared following two routes. The first

* *Present address*: School of Mechanical & Production Engineering, Nanyang Technological University, Nanyang Avenue, Singapore 63 9798, Singapore.

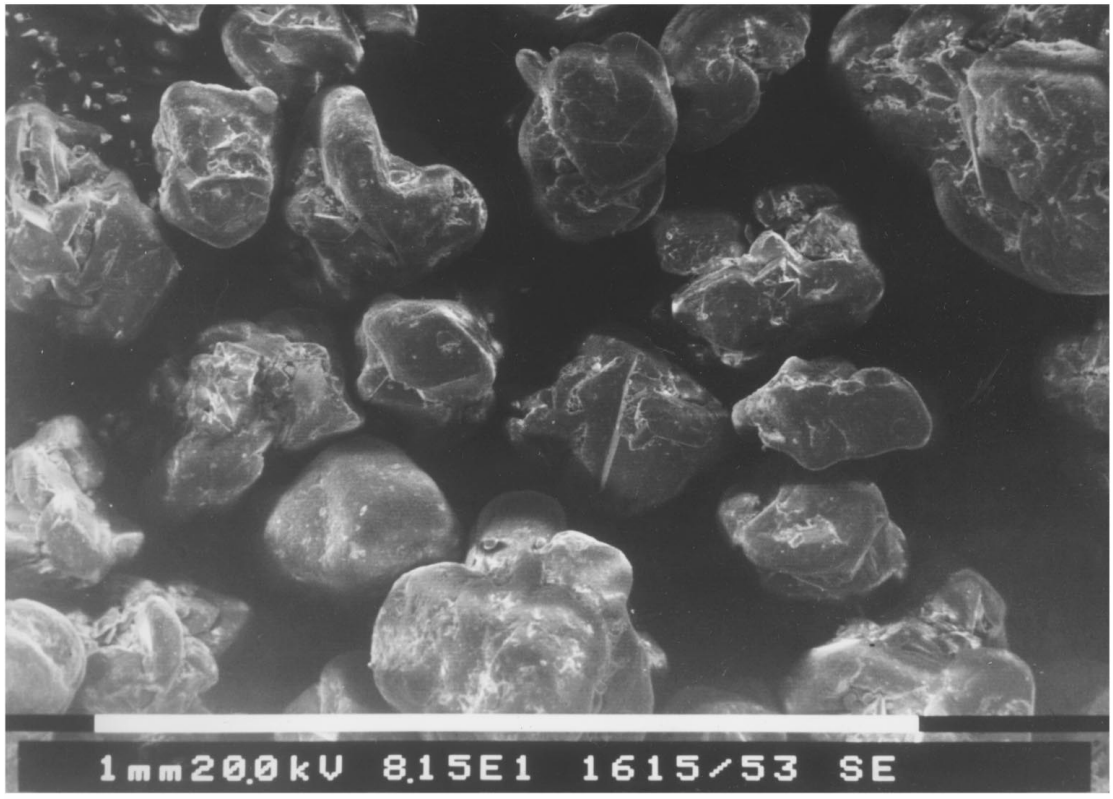

(a)

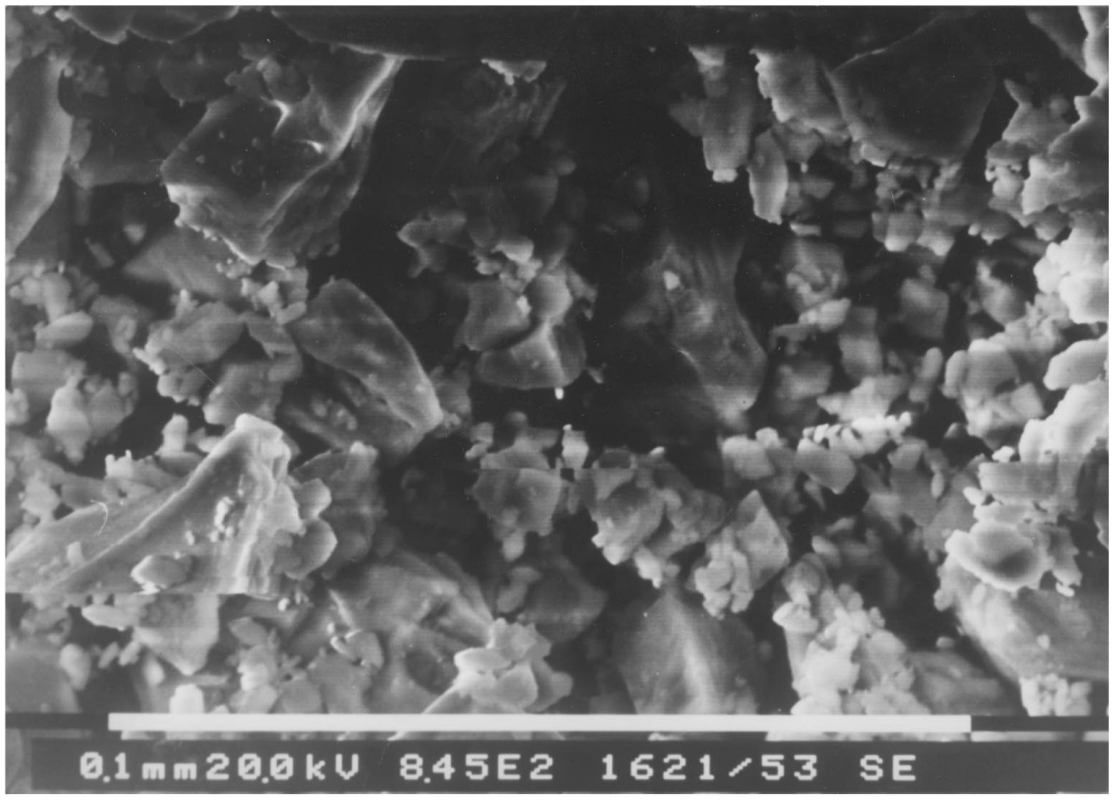

(b)

Figure 1 The morphology of salt particles: (a) K_2TiF_6; (b) KBF_4.

was to put block pieces of the commercial pure aluminium and the alloying element together in a crucible and melt them in a furnace prior to the addition of the salts. The second was that, after melting the commercial pure aluminium, the alloying elements (mixed together with the particulate salts) were added in powder form.

2.2. Preparation of the samples

2.2.1. Commercial pure Al as the base metal for the synthesis of Al/TiB_2 MMCs

Experiments were carried out in a dedicated gradient and quench furnace (Oyten) with three heating zones that can be controlled independently. With this furnace,

samples can be treated in a flowing protective atmosphere at a temperature up to 1100°C. Besides slow cooling, quenching in water can be easily done.

For each sample, a mixture of salts $K_2TiF_6 + KBF_4$ (0.6 g) was filled into a hole on the top of the Al cylinder (∼7 g). This setting ensured that Ti and B elements in the salts could diffuse into the aluminium from the top of the aluminium block during the thermal cycle. The two types of salts were mixed well with a stoichiometric ratio to form TiB_2.

The samples consisting of aluminium and salts were melted and solidified in a graphite cylindrical crucible in flowing Ar atmosphere with holding temperature, holding time, heating rate, temperature gradient and cooling rate as parameters. The inner-wall of the crucible was coated with BN to avoid a reaction between the sample and the graphite. Fig. 2 schematically shows the experimental set-up. The thermocouples were placed in the graphite crucibles to get the temperatures as closely as possible to those in the melts. Heat should be produced when the two salts react in the molten aluminium. However, the temperature profiles of the melts showed no clear sign about any resultant temperature rising. The possible reasons for that are as follows: the amount of salts used in this study and thus the heat generated by the reaction were limited; the thermocouples were not really in the melts.

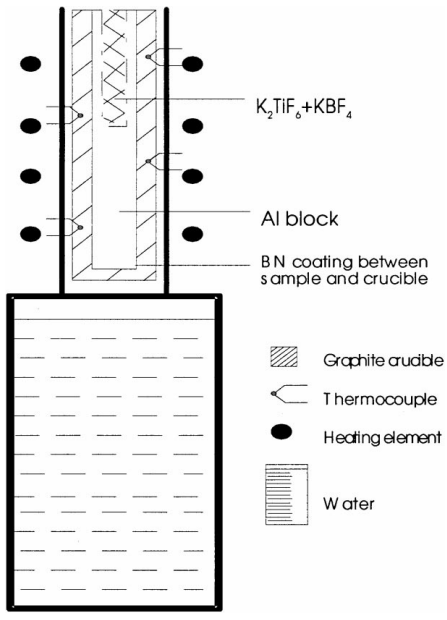

Figure 2 A schematic drawing of the experimental set-up.

For studies with temperature gradient as the parameter, we also used a furnace named ASPF (advanced solidification processing facility), which allowed us to have a high temperature gradient.

The performed experiments are summarised in Tables I and II.

2.2.2. Binary Al alloys as the base metal for the synthesis of Al/TiB_2 MMCs

The experiments were carried out with a resistance-heated furnace. The molten Al or Al alloys were first prepared in a crucible in the furnace at a certain temperature. Then, the crucible was taken out of the furnace and the oxide layer was briefly skimmed with an Al_2O_3 rod. Immediately thereafter, the salts or salts+alloying elements were added at the top of the molten metal. For each test, the aluminium was seven times the weight of the salts, and the two salts were in the stoichiometric ratio for the formation of TiB_2. The crucible was then put back in the furnace and kept there for 20 minutes. The thermocouple, which was used for measuring the temperatures, was placed touching the outer-wall of the crucible in the furnace. The composite materials cooled down and solidified in air outside the furnace. Table III gives a summary of the tests performed.

2.3. Evaluation of the castings

After each solidification process using the commercial pure Al as the base metal, the second phase particles were extracted from the aluminium matrix by dissolving the matrix material in 75 ml methanol + 3 g iodine + 3 g L(+) tartaric acid [2].

The particles were examined by XRD (Philips vertical goniometer; generator: PW1010; Cu-K_α X-ray radiation) for phase determination.

The samples were etched in Kellers (HF 1 ml + HCl 1.5 ml + HNO_3 2.5 ml + H_2O 95 ml) with a duration of 10 seconds. The microstructure was then characterised by light optical microscopy (LOM) and SEM with an EDS facility (Philips 515 and FEG 30).

In the study about the effects of temperature gradient on the product microstructure, the areas of the second phase distributed regions in the products were measured using an image analysis system in order to compare the distribution.

In the study about the distribution improvement by using binary Al alloy as the base metal, the microstructures of the products were also examined with LOM and SEM with an EDS facility (Philips 515 and FEG

TABLE I Experiments with holding temperature, holding time, heating rate and cooling rate as parameters

Sample ID	Heating rate (°C/min.)	Holding temperature (°C ± 10°C)	Holding time (min)	Temperature gradient (°C/cm)	Cooling
1	15	810	10	∼0 (Isothermal)	Quenching in water
2	15	810	35	∼0 (Isothermal)	Quenching in water
3	15	810	120	∼0 (Isothermal)	Quenching in water
4	15	810	10	∼0 (Isothermal)	Furnace cooling
5	15	910	35	∼0 (Isothermal)	Quenching in water
6	15	810	35	∼0 (Isothermal)	Furnace cooling
7	15	1010	35	∼0 (Isothermal)	Quenching in water
8	15	810	300	∼0 (Isothermal)	Quenching in water
9	30	810	35	∼0 (Isothermal)	Quenching in water

TABLE II Experiments with temperature gradient as parameter

Sample ID	Sample preparation	Sample temperature during holding (±10°C)	Temperature gradient	Area of the second phase distributed region(s)
10	Heated to 910°C at 15°C/min; after holding for 35 min, quenching in water; Oyten furnace	Top 830°C; Bottom 910°C	−12.3°C/cm[a]	∼97 mm^2
11	Heated to 910°C at 1000°C/h;	Top 906°C; Bottom 623°C	47.2°C/cm[b]	∼118 mm^2
12	After holding for 30 min, quenching	Top 710°C; Bottom 643°C	11.2°C/cm[b]	∼114 mm^2
13	In liquid Ga-In alloy;	Top 772°C; Bottom 654°C	19.7°C/cm[b]	∼111 mm^2
14	ASPF furnace	Top 896°C; Bottom 343°C	92.2°C/cm[b]	∼100 mm^2

[a]The temperature decreases from the bottom to the top of the sample.
[b]The temperature decreases from the top to the bottom in the sample.

TABLE III A list of the experiments with respect to the distribution improvement of TiB_2

Sample ID	Alloy composition	Comments	Temperature (°C)
M0629	Al-0.8wt%Mg	Mg-powder	810
M0637	Al-9.1wt%Mg	Mg-powder	860
M0630	Al-9.1wt%Sb	Sb-block	810
M0638	Al-2.7wt%Sb	Sb-block	860
M0631	Al-10wt%Mn	Alloy available	860
M0632	Al-1.0wt%Cu	Cu-powder	860
M0633	Al-9.1wt%Cu	Cu-powder	860
M0635	Al-9.1wt%Zn	Zn-block	860
M0636	Al-3.8wt%Fe	Fe-block	860
M0639	Al-9.1wt%Cr	Cr-powder	860
M0634	Al-12wt%Si	Alloy available	860
M0641	Al-5wt%Si	Alloy made by diluting Al-12wt% Si	860
M0642	Al-2wt%Si	Alloy made by diluting Al-12wt% Si	860
M0640	pure Al	As a reference	860

30). XRD was used for determining the phases when necessary.

3. Results and discussions

3.1. Characterisation of Al/TiB_2 products

During the heat-treating, the elements Ti and B were expected to be introduced from K_2TiF_6 and KBF_4 respectively into the molten aluminium and to react within it. Since these two types of salts were mixed stoichiometrically to form TiB_2, TiB_2 was supposed to be the only intermetallic phase formed by the reaction. The XRD analyses confirm this (Fig. 3). The following reaction formula [3] may therefore be relevant:

$$3K_2TiF_6 + 6KBF_4 + 10Al \rightarrow 3TiB_2 + (9KAlF_4 + K_3AlF_6) \quad (1)$$

Strings as well as clusters of particle agglomerates are distinct microstructural features generally found in all the products (Fig. 4). EDS combined with XRD results proves that they consist of (Ti, Al)B_2 particles. That means, there is always some Al analysed on the sites of TiB_2. The understanding about the incorporation of Al into TiB_2 lattice was reported earlier in [4]. Furthermore, some black dots are also visible in Fig. 4 and EDS analysis confirms that they mostly came from the slags.

In general, the diboride particles formed are very fine, with a size up to 1 μm. They form agglomerates of different sizes. Large groups of agglomerates together form a cluster type structure. The large specific surface area of small particles may play an important role for the agglomeration. It is found in the present study that larger particles tend to form smaller agglomerates possibly due to their smaller specific surface area. The same consideration applies to the strings as well. Furthermore, the relatively large diboride particles (up to ∼1 μm) in both clusters and strings show well developed crystal boundary (typically hexagonal in cross-section).

3.2. Effects of processing parameters on product microstructure

The phase distribution once formed can be modified by the solidification process. When a melt containing

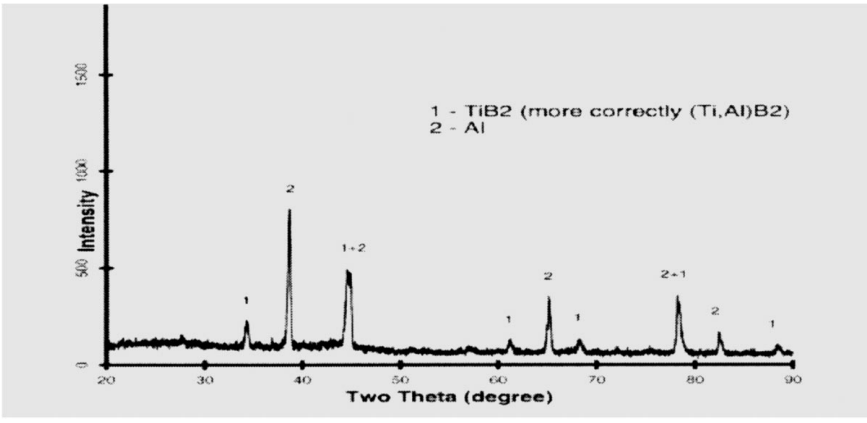

Figure 3 XRD pattern of the particles extracted from a composite sample (commercial pure Al as the matrix). It clearly shows that TiB_2 (more correctly (Ti, Al)B_2) is the only ceramic phase formed by the reaction between salts within molten aluminium. XRD analyses for other composite samples (commercial pure Al as the matrix) give the same result.

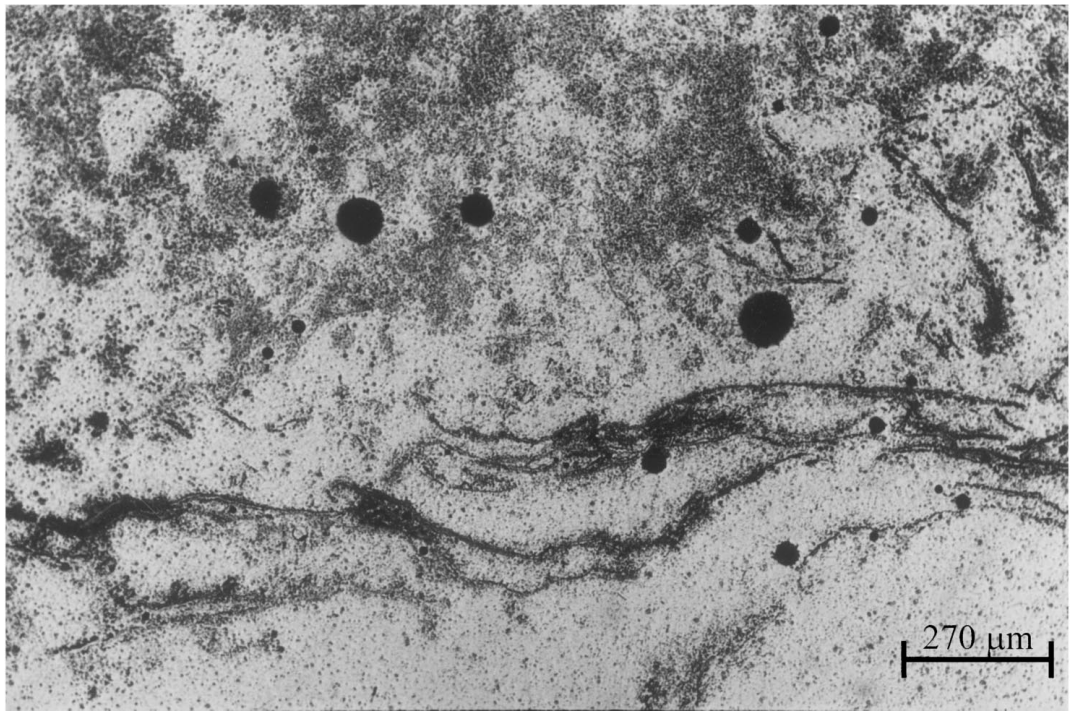

Figure 4 Diboride particles appear as strings or clusters of particle agglomerates (Sample 7). These typical distinct microstructural features are generally found in every composite sample (commercial pure Al as the matrix).

a distribution of second phase particles solidifies, the initial distribution of the particles can change due to three phenomena, namely, buoyant motion of the particles, pushing of the particles by the moving solidification front, and by convection current in the melt [5]. Theories for particle pushing predict that there is a critical velocity of the solidification front, below which the front pushes the particles along with it. Above the critical velocity, the front grows around the particles and engulfs them. The critical velocity is a function of the particle size and the temperature gradient at the solidification front [6].

3.2.1. Influence of holding temperature

Increasing the holding temperature from 810°C to 1010°C, hardly changes the microstructure of composite product (Samples 2, 5 and 7).

The morphology and size of the diboride particles does not vary clearly (if any) with holding temperature. However, it seems that more particles might have developed to a size nearer to ∼1 μm and their crystal boundaries are accordingly better developed as the temperature increases (Fig. 5). Fig. 5 shows that the diboride particles remain below 1 μm in size when the temperature increases from 810°C to 1010°C. This is likely because, the temperatures used in the present study may not be high enough for a visible growth of TiB_2 to occur. Evidence from literature proves that at 1500°C and 10 hours, TiB_2 crystal could grow to 5000 μm in cross section from an alloy of Al-8.8%Ti-3.6%B which is slightly over-stoichiometric (Ti/B = 2.4) [7]. Also, as reported earlier in [8], a distribution of (Ti, Al)B_2 particles of up to 2–3 μm was formed in Al matrix by heating Al-TiO_2-B to 1400°C and keeping at that temperature for 20 minutes prior to the cooling in the furnace.

The fine sizes (below ∼1 μm) of diboride particles formed in the Al matrix suggest that for this phase nucleation is easier than growth. This might be related to the Al incorporation in the TiB_2 lattice. Youdelis [9, 10] has shown, by classical nucleation theory, that the nucleation rate increases exponentially with the square of the nucleation entropy; the nucleation entropy increases with the number of alloying components, which concentrate in the nucleating phase. Thus the incorporation of even small amount of Al into TiB_2 should increase the nucleation rate considerably, and the particle size would decrease correspondingly.

3.2.2. Influences of holding time

Prolonging holding period from 10 up to 300 minutes does obviously not change the microstructure (Samples 1, 2, 3 and 8). However, the network distribution of TiB_2 is visible at some places in Samples 2, 3 and 8 and it is less clear in Sample 1 (Fig. 6). This might mean that the critical velocity for particle pushing increases as the holding time is prolonged. This finding might be an evidence that boride particle agglomerates tend to be slightly disintegrated as holding continues, which is not contradictory with the careful LOM observations.

3.2.3. Influence of cooling rate

Samples 4 and 6 were cooled down in the furnace. During the solidification of these samples, the velocity of the solidification front is below its critical value because of the slow cooling. Subsequently the particles were pushed by the solidification front and thus network structures of the distribution were dominant (Fig. 7).

(a)

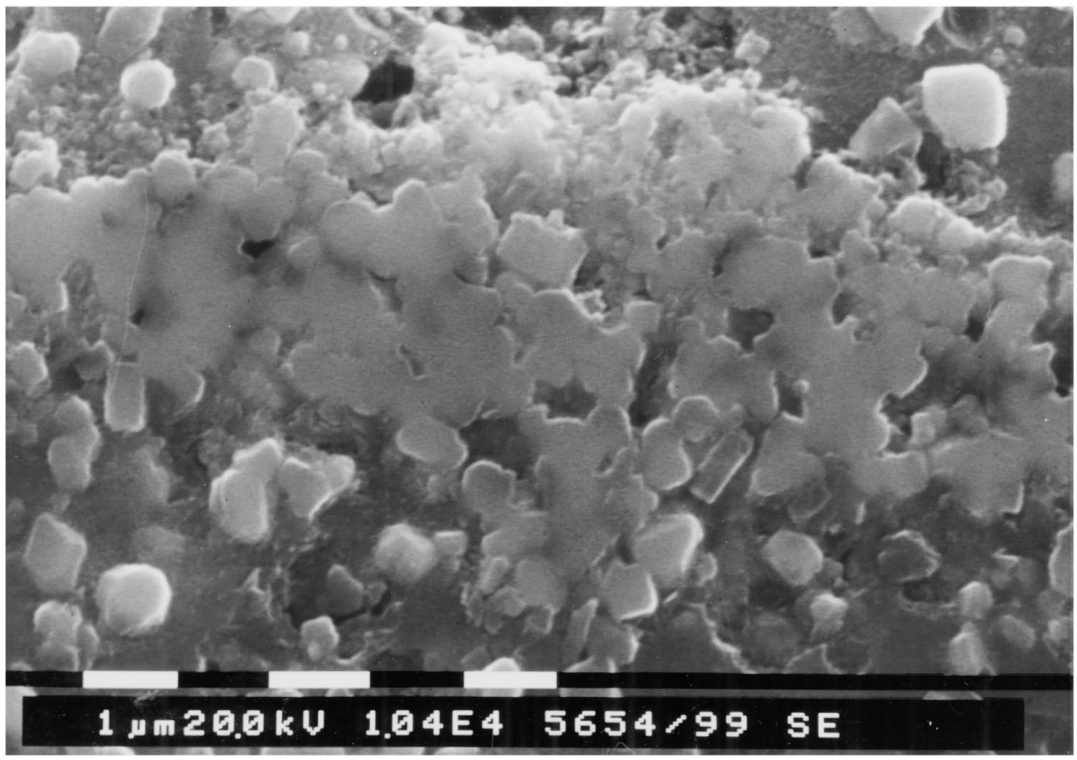

(b)

Figure 5 The diboride particles remain submicron in size when the temperature increased from 810°C to 1010°C: (a) 810°C; (b) 1010°C.

3.2.4. Influence of heating rate

Samples 2 and 9 differ in the heating rate (15°C/min versus 30°C/min). No microstructure difference is observed between these two samples. This is likely because that the difference of the two heating rates is quite low; however, a higher heating rate is difficult to achieve with the available furnace. On the other hand, the effects of heating rate could be reflected by the effects of holding temperature and holding time; due to slow kinetics of the microstructural change resulted from varying temperature and time, it is not surprising that the small difference of heating rate (15°C/min) does not lead to a visible change in the microstructure.

3.2.5. Influence of temperature gradients

Samples 10 to 14 were meant to assess the effects of the temperature gradient (from −12.3°C/cm to +92.2°C/cm) on the microstructure of the final composite product.

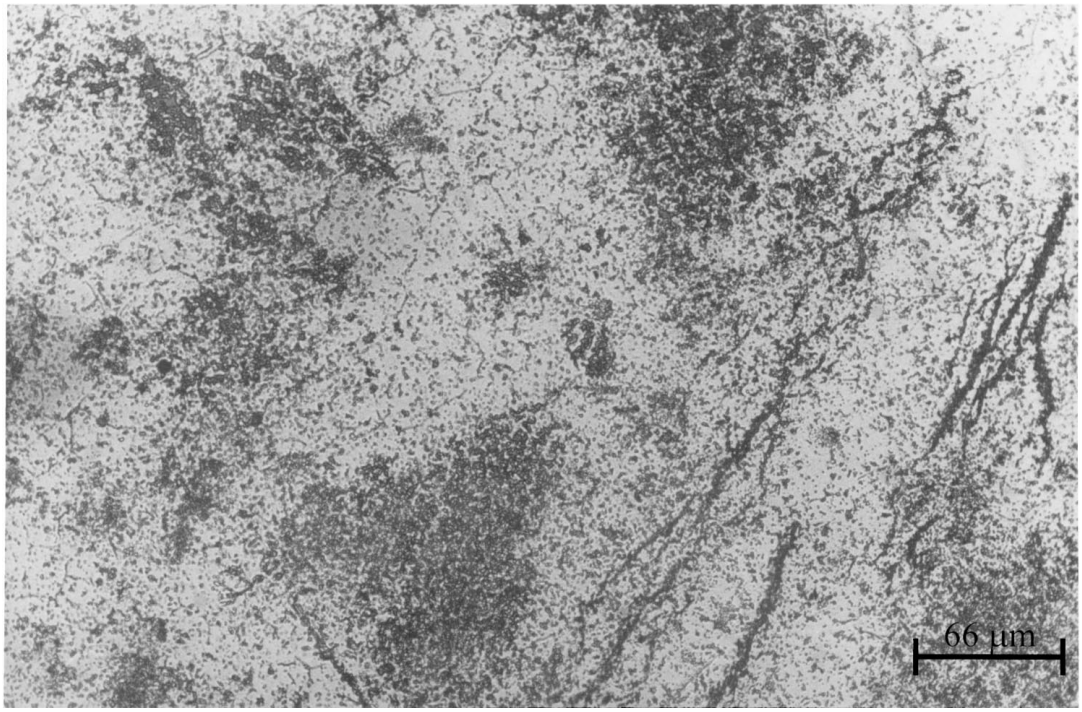

(a)

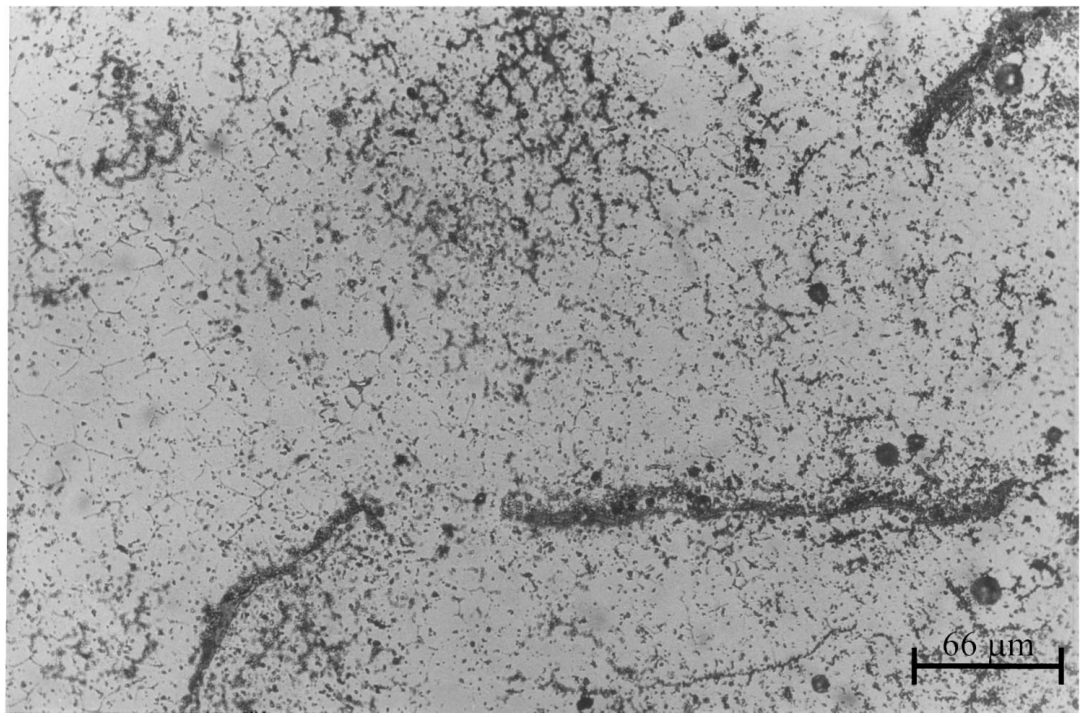

(b)

Figure 6 Diboride particles tend to be distributed along grain boundaries as the holding prolonged from 10 to 300 minutes: (a) 10 min; (b) 35 min; (c) 120 min; (d) 300 min. (*Continued*.)

The composite samples consist of particle-rich and particle-free regions. The particle-rich regions are generally bordered with TiB_2 strings and the regions are clearly visible macroscopically after polishing (even without etching). The areas of particle-rich regions in the composites, measured by quantitative image analysis, are given in Table II. It can be seen that the temperature gradient has little influence on the area value of particle-rich regions. In other words, the temperature gradient hardly affects the distribution of TiB_2 particles in the Al matrix.

There are two directions for the temperature gradients in a sample: a positive one (temperature increases from the bottom of the sample to the top of the sample) and a negative one (temperature decreases from the bottom of the sample to the top of the sample). A negative temperature gradient would lead to a forced natural convection. However, the results indicate that -12.3°C/cm is obviously not high enough to create a convection current that would be sufficient to achieve a visible distribution improvement. On the other hand, a positive temperature gradient will not lead to a

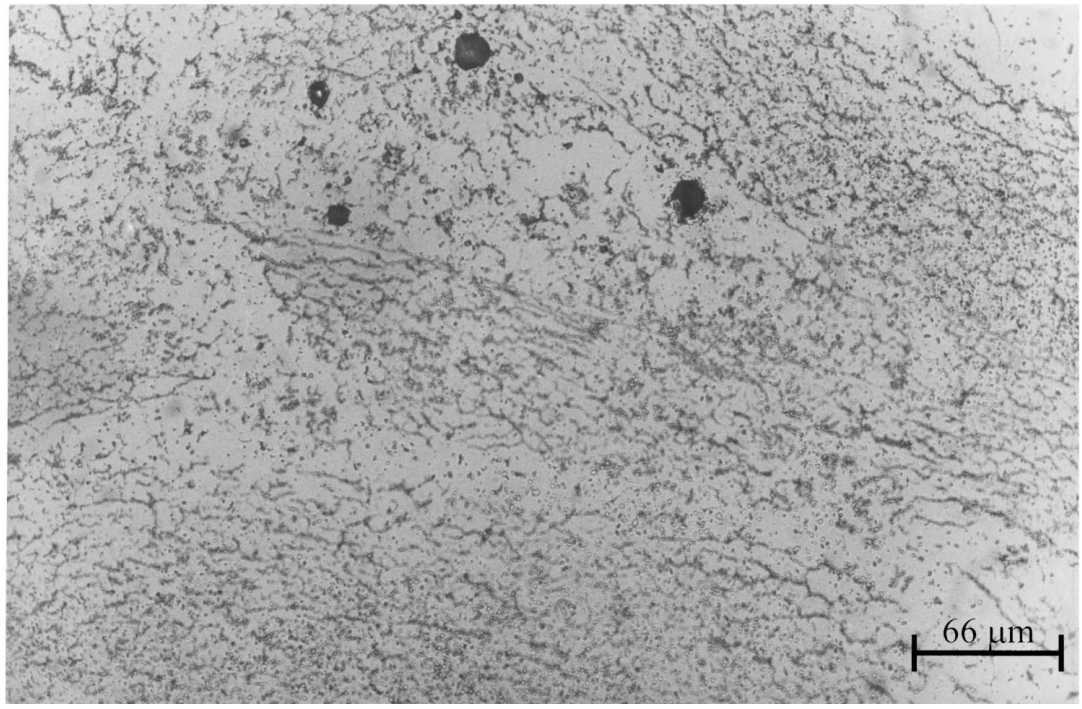

(c)

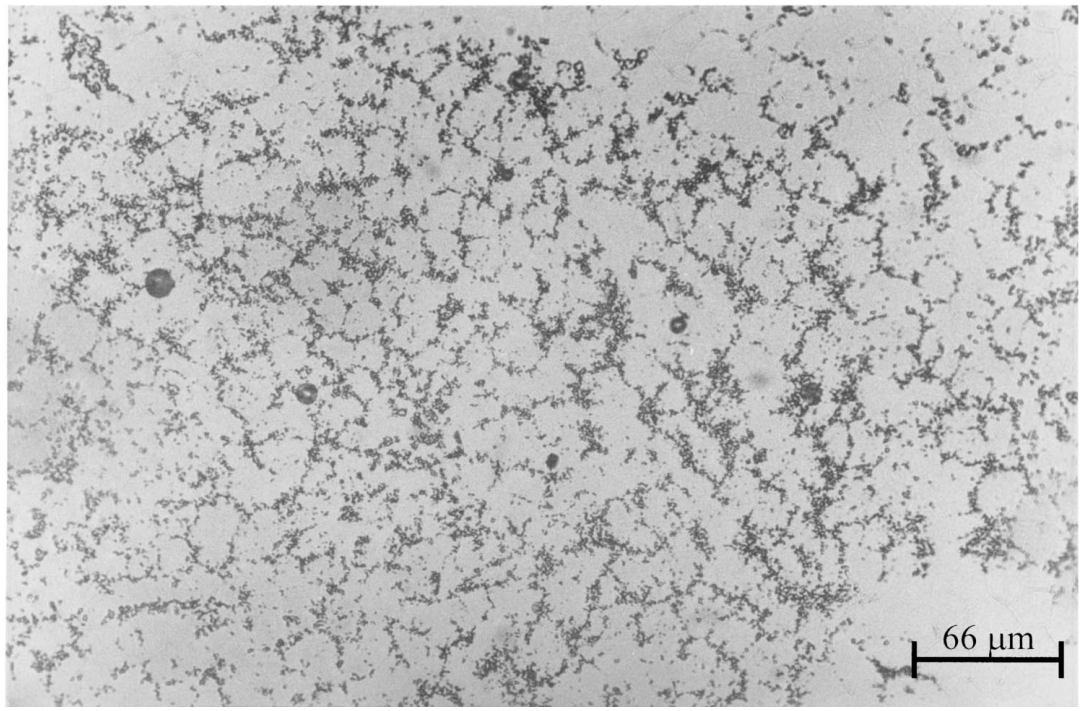

(d)

Figure 6 (*Continued*.)

convection current. From the results we have indeed seen that no distribution improvement is achieved by applying a positive temperature gradient.

Moreover, it was thought that for a positive temperature gradient the second phase particles should generally be located at the bottom of the sample due to sedimentation; similarly, for a negative one, if the convection force is not strong enough, the second phase particles should generally also be found at the bottom of the sample. Both of the cases were indeed observed in our experiments (Sample 10—negative temperature gradient; Sample 11—positive temperature gradient). However, due to some other practical reasons such as macroscopical holes which can prevent the second phase particles from sinking, the second phase distributed regions are sometimes found in the upper part of the samples.

3.2.6. Role of liquid Al

The question arises whether a molten medium like aluminium melt is essential for the formation of TiB_2. In an experiment, a powder mixture of $K_2TiF_6 + KBF_4$ was

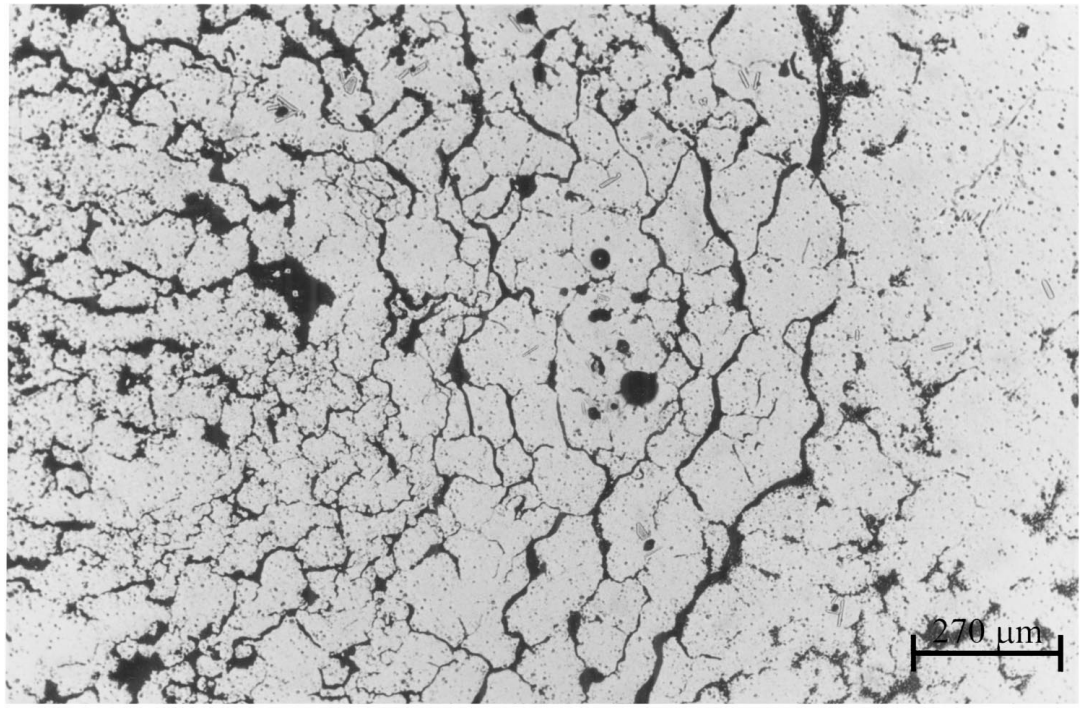

(a)

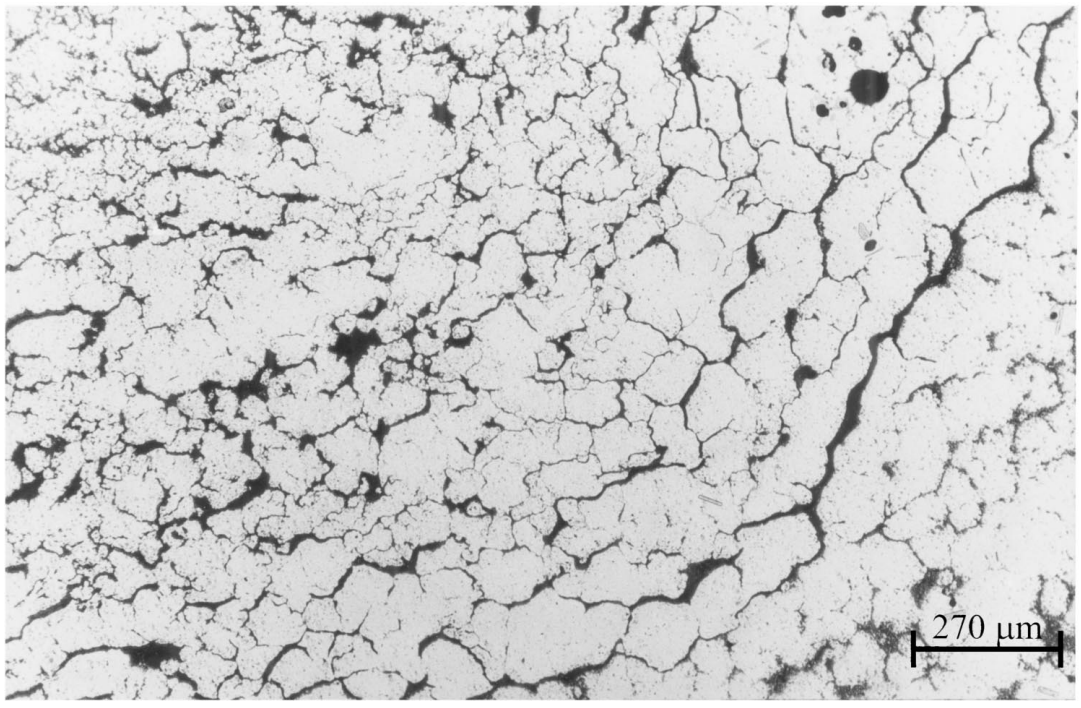

(b)

Figure 7 After slow cooling (furnace cooling), network structures are dominant. (a) Sample 4; (b) Sample 6.

heated to 810°C and held at that temperature for 35 min in a closed air environment in a resistance-heated furnace. The powders of the two types were mixed well with a ratio corresponding to TiB_2. The salts were in molten state at this temperature. After resolidifying, the product was checked by LOM and XRD analysis: no TiB_2 phase was found.

By another experiment, we checked whether liquid Ag could be used instead of Al as the medium for the formation of TiB_2. In this experiment, the above-mentioned salts mixture was put on the top of Ag block in a crucible and they were heated up to 1010°C. Microstructural comparison was made between the product and the starting Ag by means of LOM, SEM and EDS, and no difference was observed. In other words, the salts did not go into the Ag matrix and no second phase was found in the Ag matrix. Indeed, after the experiments the salts and the silver block were clearly separated.

The results of the two complementary experiments support the proposed reaction mechanisms responsible for the formation of TiB_2. It corresponds to the reaction

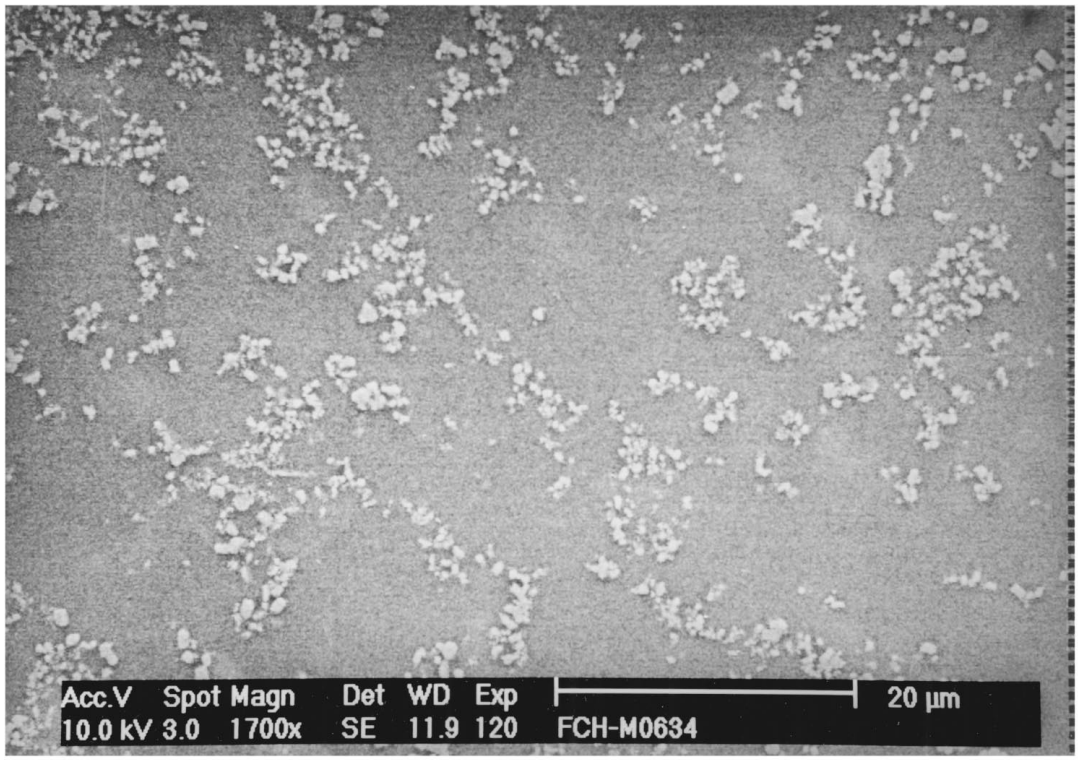

(a)

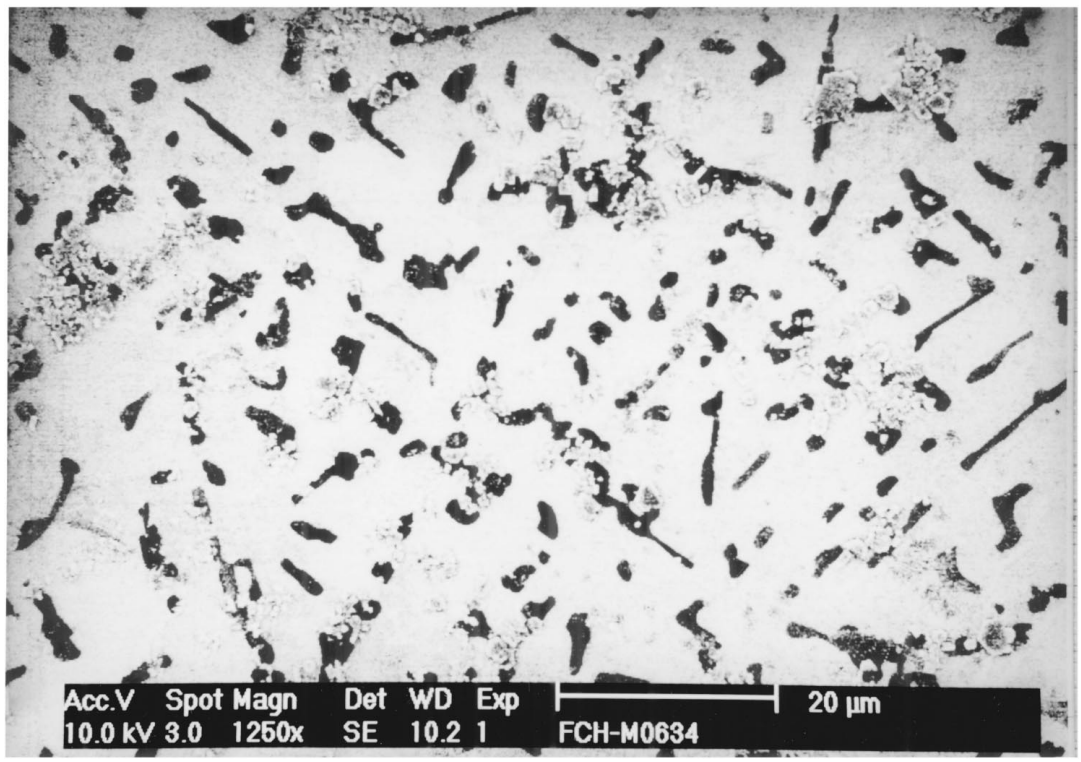

(b)

Figure 8 A uniform dispersion of TiB_2 in the Al-12wt%Si matrix: (a) Sample with a silver coating (no contrast between Si and Al); (b) sample with no coating (Al is white; Si is dark).

mechanisms as described in Ref [3]. Initially the following reactions take place:

$$3K_2TiF_6 + 13Al \rightarrow 3Al_3Ti + 3KAlF_4 + K_3AlF_6 \quad (2)$$

$$2KBF_4 + 3Al \rightarrow AlB_2 + 2KAlF_4 \quad (3)$$

$KAlF_4$ and K_3AlF_6 are the slag phases that have to be separated from the composite. Al_3Ti and AlB_2 once formed almost immediately react to form TiB_2 in the Al matrix according to the following formula:

$$Al_3Ti + AlB_2 \rightarrow TiB_2 + 4Al \quad (4)$$

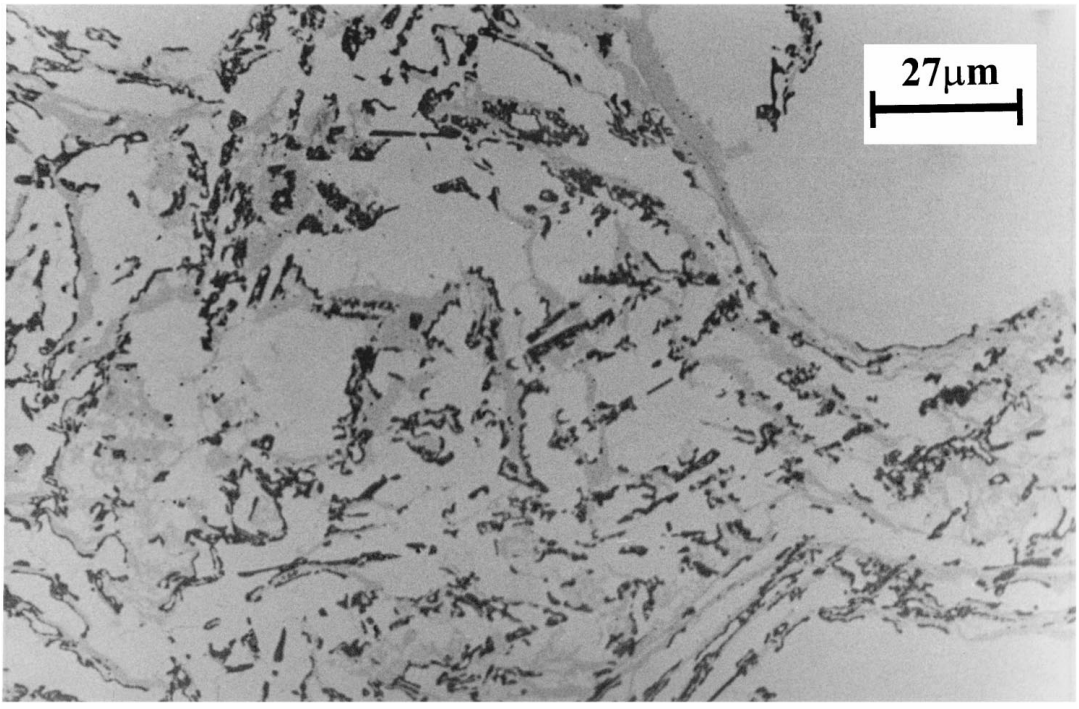

(a)

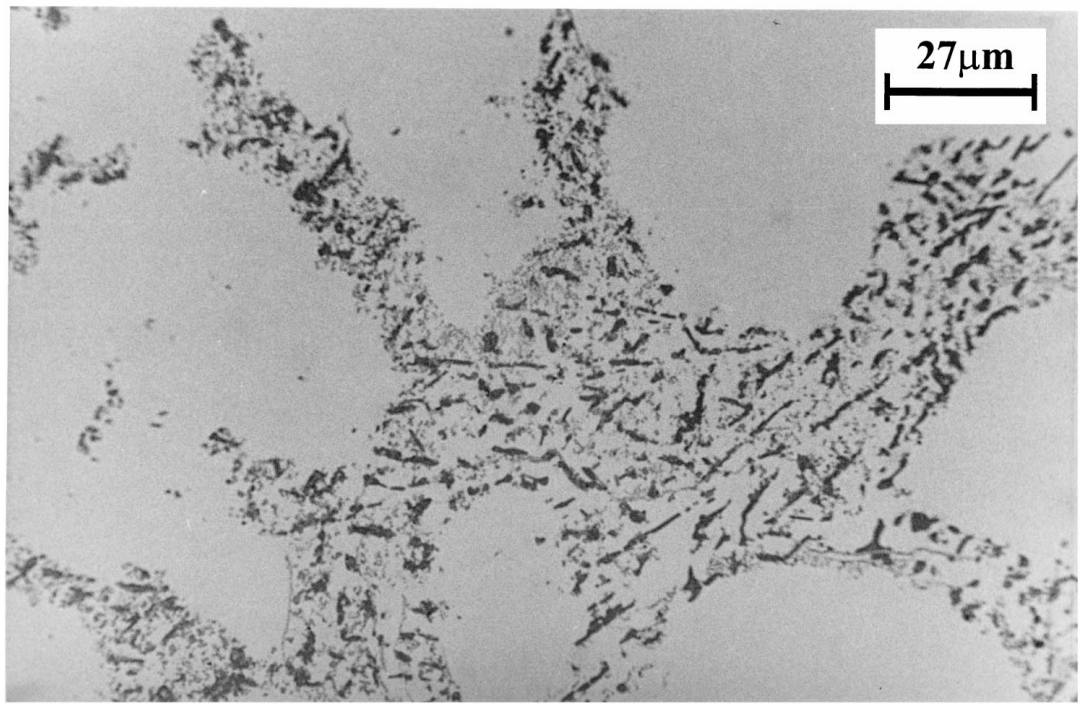

(b)

Figure 9 Typical microstructures of (Al-5wt%Si)/TiB_2 MMCs: (a) Strong TiB_2 agglomerates/strings still remain; (b) regions in which TiB_2 particles are more discretely distributed are also found due to varying local distribution and solidification conditions.

As can been seen Al is essentially involved in the reactive process for the formation of TiB_2.

3.3. Improvement of the distribution of TiB_2 in the Al matrix

The best results were obtained when Al-12wt%Si was used as the matrix. A homogenous distribution was typically found in the microstructure (Fig. 8) although small TiB_2 agglomerates/strings could be occasionally found. It was confirmed by XRD and EDS that the fine particulates (bright) and lamellae (dark), shown in Fig. 8, were TiB_2 and Si respectively. It is also noticed from the microstructure that TiB_2 particles are in contact with Si lamellae. It is clear that the distribution of TiB_2 has been greatly improved by using Al-12wt%Si as the matrix in comparison with the case that pure Al is used as the matrix.

Al-12wt%Si is the eutectic composition of the Al-Si alloy. It is an important eutectic casting alloy, typically having a lamellae microstructure [11]. Unlike the solidification of single-phase primary crystal, during

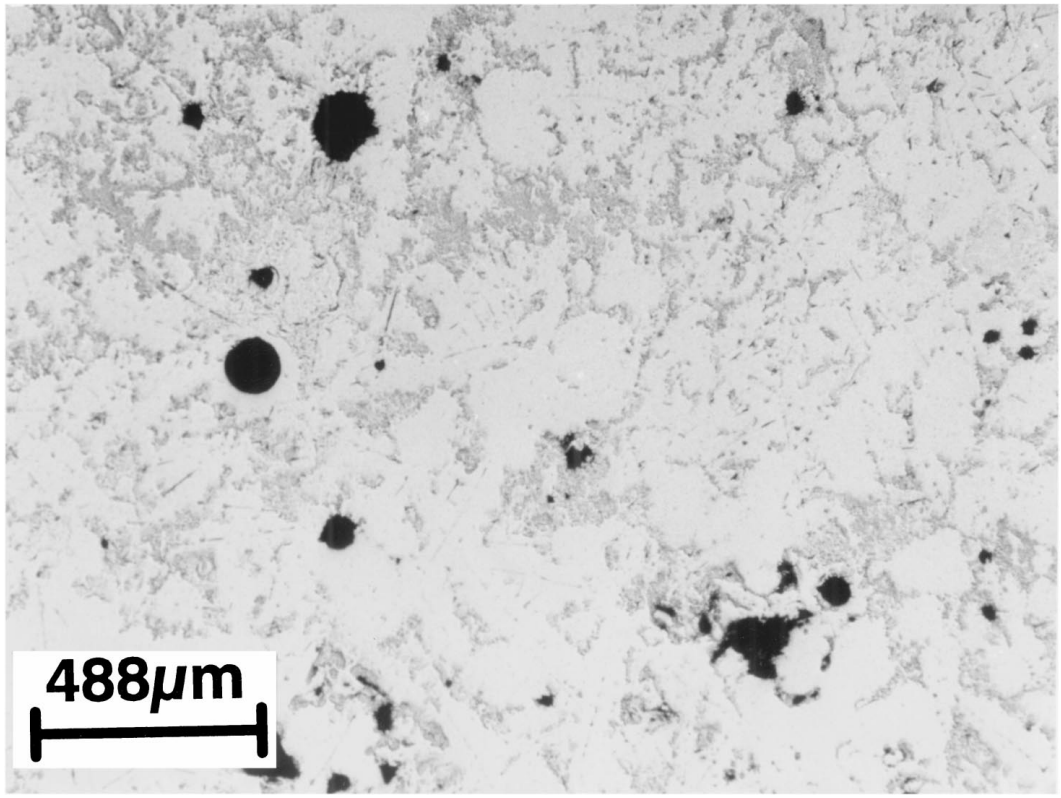

Figure 10 TiB_2 distributed in an Al-Sb alloys (Al-9.1wt%Sb).

the Al-Si eutectic solidification, TiB_2 particles would be entrapped in a grain between the eutectic cells. In the solidification of single-phase primary crystal, compared to the eutectic solidification, more TiB_2 particles could be pushed by the solidification front to the interfaces of solid-liquid aluminium. Hence, the good distribution of TiB_2 by using Al-12wt%Si as matrix most likely results from the fine eutectic structure of the Al-Si alloy. On the other hand, a eutectic composition is preferred for casting alloys, because of their excellent casting behaviour and the interesting composite properties after solidification [11]. Accordingly, further efforts are worthwhile to be made to further improve the current results in order to achieve useful metal matrix composites with TiB_2 homogeneously distributed in an Al-Si eutectic matrix.

Further improvement of the dispersion results might be expected if the following measures would be applied for the casting:

- use a structure refining element like strontium to achieve a still finer Al-Si eutectic structure. Rooy states that Sr can be used to modify the Al-Si eutectic and a very low addition level can result in an effective modification [12]. In addition, a small amount of Na salt addition may also modify the Al-Si eutectic in this respect [13].
- use a faster cooling to prevent the pushing away of TiB_2 by the solidification front.
- use mechanical stirring or another efficient stirring means when casting.

Compared to the Al-Si eutectic alloy, Al-Si alloys with lower Si contents do not lead to such good results. Taking Al-5wt%Si as an example, when the alloy solidifies, Al first nucleates and grows as a dendrite. As TiB_2 particles are pushed by the solidification front, more and bigger agglomerates/strings are formed and located in the interdendritic regions. Therefore, once the eutectic temperature is reached, more TiB_2 particles would already exist as agglomerates or strings, and the remaining liquid space for the eutectic structure is already small. Finally the big TiB_2 agglomerates or strings are in the last solidified limited spaces surrounded by primary Al(Si) phase (Fig. 9a). However, compared to pure Al matrix, the off-eutectic Al-Si alloys here still correspond to better TiB_2 dispersion, since the TiB_2 particles are more discrete in some regions (Fig. 9b). Furthermore, 5 wt% and 2 wt% of Si contents in the alloys do not give obvious differences concerning the TiB_2 dispersion. The reason might be that the compositional differences are not large enough to result in a clear microstructural difference. Additionally, microscopic observations indicate that, particles which are more discrete have a bigger particle size.

In Al-Sb alloys as matrix material, agglomerates and strings are still more or less distinct microstructural features. However, compared to pure Al as the matrix, Al-Sb alloys as the matrix materials correspond to smaller sizes of TiB_2 agglomerates and strings (Fig. 10). The slight improvement of TiB_2 distribution in Al-Sb alloys most likely comes from the grain refining effect of Sb, which is in agreement with literature [14]. As a small quantity of Sb addition would normally suffice for a grain refining purpose, a higher Sb content in Al may not help to further improve the distribution. On the other hand, higher Sb contents in Al may lead to the formation of intermetallic Al-Sb.

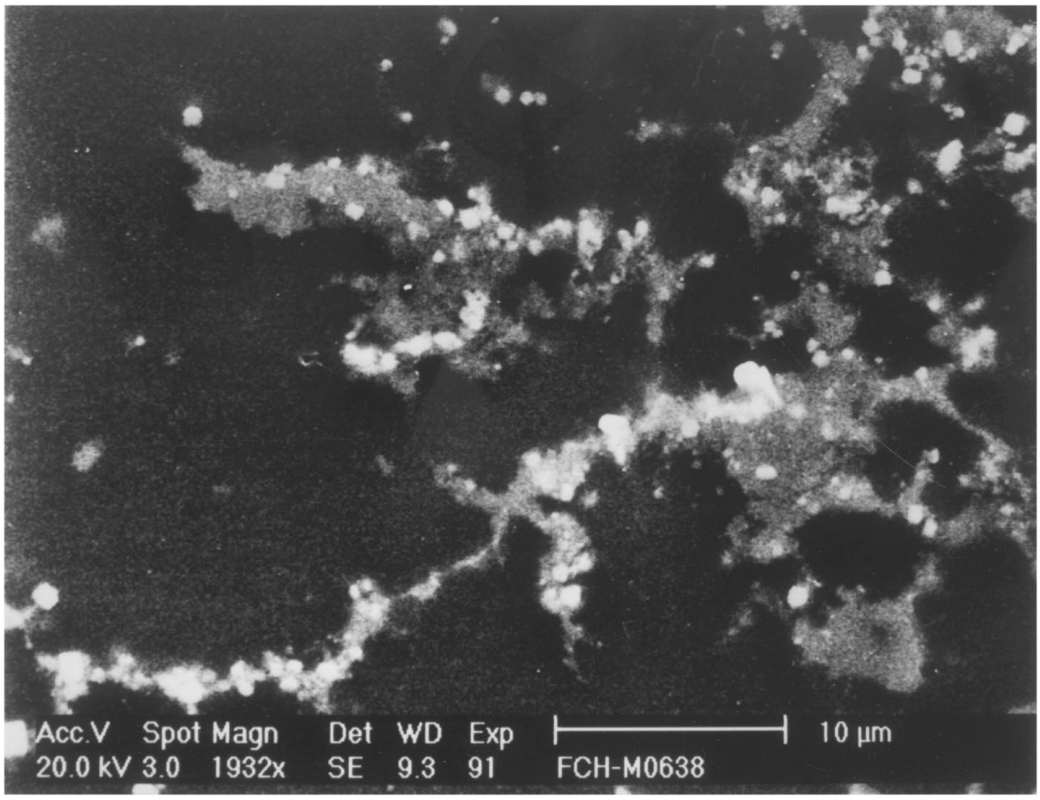

Figure 11 The AlSb phase (bright) in the Al-AlSb eutectic structure exists as small particulates.

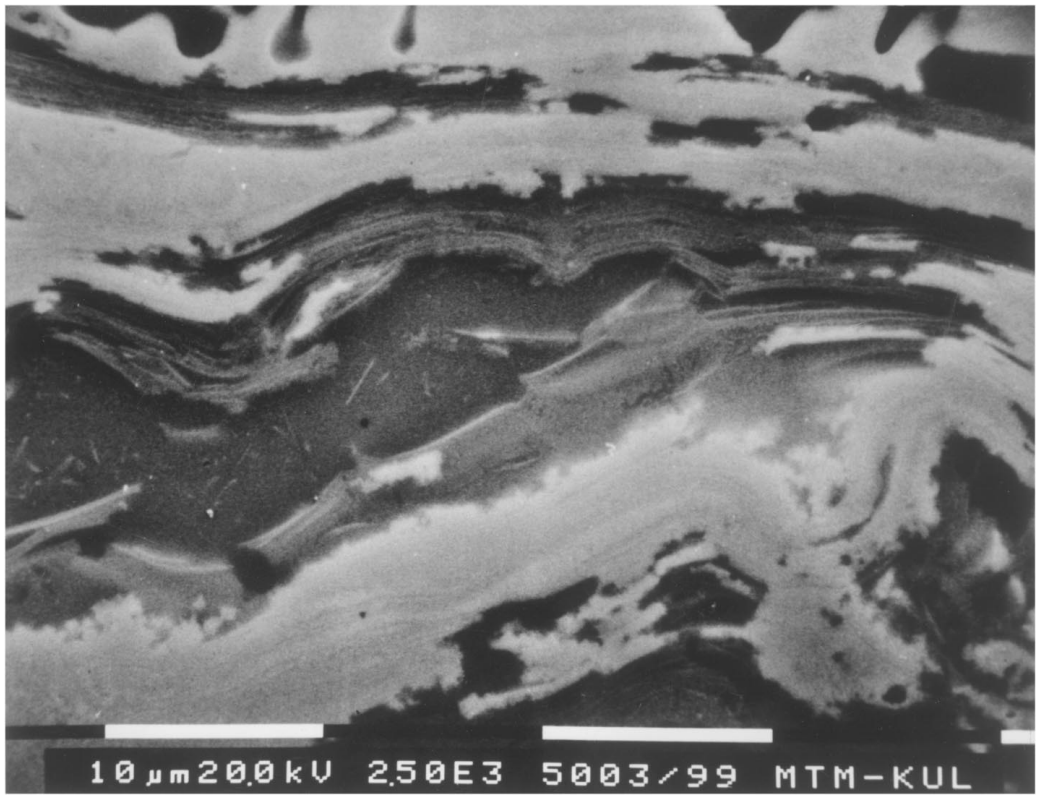

Figure 12 The thick laminar intermetallic (θ) phase (bright), Al_2Cu, overlaps with TiB_2 strings (dark).

Al-Sb alloys also have an eutecticum. However, the eutectic solidification does not lead to a good distribution of TiB_2, probably because of the different eutectic structure as compared to that in Al-Si alloys. The Al-Sb phase (bright) in the Al-Sb eutectic structure exists as small particulates (Fig. 11). The particulates are seen to be in contact with TiB_2 agglomerates as the nucleation of Al-Sb is likely easier there.

The other investigated alloying elements are Mg, Mn, Cu, Zn, Fe and Cr (Table III). None of these leads to an improved distribution of TiB_2. They do not form fine laminar eutectic structures or have no grain refining

effects for the Al matrix. The use of Al-9.1wt%Cu as the matrix, for example, even leads to poorer distribution of TiB_2. The intermetallic (theta) phase, Al_2Cu, formed during solidification are thick lamellae overlapping with TiB_2 strings (Fig. 12); and they are located in the inter-dendritic regions, which will have negative effects on the mechanical properties of the composite products.

4. Conclusions

Al/TiB_2 MMCs have been successfully produced by a reaction between stoichiometrically mixed K_2TiF_6 and KBF_4 salts to form reinforcing TiB_2 particles within molten Al matrix. Strings as well as clusters of particulate agglomerates are distinct microstructural features for all the composites with pure Al as the matrix.

Increasing holding temperature from 810°C to 1010°C, prolonging holding time from 10 to 300 min, changing heating rate from 15 to 30°C/min, applying a temperature gradient or using slow cooling (furnace cooling) instead of quenching hardly affects the growth kinetics of the diboride phase. The nucleation of this phase is much easier than the growth, resulting in the fine size of diboride particles (below $\sim 1\ \mu$m under current conditions). Both strings and agglomerates generally contain particles near to $\sim 1\ \mu$m in size as well as a large amount of extremely fine particles.

For quenched composites, it seems that a network distribution tends to be formed when the holding lasts. This might imply that the agglomerates and strings of diboride particles tend to be slightly disintegrated when holding. For slowly cooled samples, the particles are pushed by the solidification front and therefore network structures are dominant.

TiB_2 cannot be formed by reactions between salts alone without an other medium. Molten aluminium can be such a medium but molten silver cannot.

Dispersion of TiB_2 particles in Al is improved by adding Si to the matrix. A homogeneous distribution of TiB_2 is obtained when a eutectic Al-Si alloy is used. It is expected that the results might be further improved by using structure-refining elements to refine the eutectic structure, by using faster cooling to prevent the pushing away of TiB_2 by the solidification front, or by applying mechanical stirring or other efficient stirring means. Furthermore, the use of Al-Si alloys with lower Si contents (5 wt% or 2 wt%) as the matrix materials does not lead to such a good distribution. Compared to Al as the matrix, Al-Sb alloys as the matrix correspond to smaller sizes of TiB_2 agglomerates/strings. The dispersion of TiB_2 in the matrix is slightly improved by Sb addition in Al due to a grain refining effect.

Acknowledgements

One of the authors (CFF) gratefully acknowledges the support of a scholarship on behalf of the PRODEX-project (DWTC).

References

1. P. DAVIES, J. L. F. KELLIE and J. V. WOOD, *Key Engineering Materials* **77–78**I (1993) 357–362.
2. M. M. GUZOWSKI *et al.*, *Metall. Trans.* **18A** (1987) 603–618.
3. J. KELLIE and J. WOOD, *Mater. World* January (1995) 10–12.
4. C. F. FENG and L. FROYEN, *Materials Letters* **32** (1997) 275–279.
5. R. SASIKUMAR and M. KUMAR, *Acta Metall. Mater.* **39**(11) (1991) 2503–2508.
6. L. VAN VUGT and L. FROYEN, *Microgravity Sci. Technol.* **X/2** (1997) 95–105.
7. I. HIGASHI, Y. TAKAHASHI and T. ATODA, *J. Crystal Growth* **33** (1976) 207–211.
8. C. F. FENG and L. FROYEN, *Scripta Mater.* **36**(4) (1997) 467–473.
9. W. V. YOUDELIS, *Metall. Sci.* **9** (1975) 464–466.
10. *Idem.*, *ibid.* **13** (1979) 540–543.
11. KURZ and D. J. FISHER, "Fundamentals of Solidification" (Trans. Tech. Publications Ltd., Switzerland, 1985) pp. 97–99.
12. E. L. ROOY, in "Metal Handbooks," 9th ed., Vol. 15: Aluminium and Aluminium Alloys (ASM International, 1988) pp. 746.
13. G. HU and M. QIAN, "Physical Metallurgy" (Shanghai Press of Science and Technology, 1980) pp. 184–185 (in Chinese).
14. T. HIKOSAKA *et al.*, *Casting Materials* **61**(11) (1989) 780–786 (in Japanese).

Received 25 February
and accepted 12 July 1999